Colloid Polym Sci (2009) 287:829–837
DOI 10.1007/s00396-009-2037-9

ORIGINAL CONTRIBUTION

Controllable fabrication of nanocrystal-polymer hybrids via the catalytic chain transfer polymerization process

Cai-Feng Wang · Yu-Peng Cheng · Ji-Yi Wang · Dong Zhang · Lin-Rui Hou · Li Chen · Su Chen

Received: 15 January 2009 / Revised: 31 March 2009 / Accepted: 2 April 2009 / Published online: 5 May 2009

Abstract A facile catalytic chain transfer polymerization (CCTP) technique has been developed to synthesize covalently linked CdS nanocrystal-polymer hybrids with good optical properties. The in situ polymerization of methyl methacrylate (MMA) on the surface of modified CdS nanocrystals (NCs) with diameter of 5 nm via CCTP process yielded CdS-polymethylmethacrylate (PMMA) hybrid nanocomposites; while the incorporation of hydroxyl-coated CdS NCs into poly(methacryloxypropyltrimethoxysilane) (PMPS)-*co*-PMMA matrices prepared by CCTP afforded CdS-PMPS-*co*-PMMA hybrid nanocomposites, which were further cross-linked by free radical polymerization to form CdS NC-polymer network. The spectroscopic studies indicate that as-prepared CdS NC-polymer hybrids show good photoluminescence (PL) and the NC-polymer network exhibits highly enhanced PL property with respect to that before cross-linking. Also described are the probable mechanism for the catalytic chain transfer polymerization on the surface of modified nanocrystal and the measurement of chain transfer constants.

Keywords CdS nanocrystal · Catalytic chain transfer polymerization (CCTP) · Grafting polymerization · Optical properties

C.-F. Wang · Y.-P. Cheng · J.-Y. Wang · D. Zhang · L.-R. Hou · L. Chen · S. Chen (✉)
State Key Laboratory of Material-Oriented Chemical Engineering, College of Chemistry and Chemical Engineering, Nanjing University of Technology, No. 5 Xin Mofan Rd, Nanjing 210009, People's Republic of China
e-mail: chensu@njut.edu.cn

Introduction

It has been recognized in recent years that semiconductor nanocrystals (NCs) possessing quantum confinement effect can exhibit size-dependent optical and electrical properties [1–4]. These materials have received considerable attention from academia and industry, owing in part to their great potential for applications as light-emitting devices [5, 6], nonlinear optical devices [7], solar cells [8, 9], lasers [10], and biological labels [11–13]. Since any of these potential applications would benefit from the use of stable NCs with desired properties, the development of the surface chemical processing of NCs has become a major research focus. One effective strategy is the preparation of nanocrystal-polymer hybrid nanocomposites by surface passivation of the NC core with capping polymer ligand [14–23]. Here, the polymer not only acts as a stabilizer to keep inherently metastable NCs kinetically stabilized, but also provides inorganic NCs with controllability of nanoparticle nucleation and growth, flexibility, solubility, diversity, and processability. Attempts to incorporate inorganic NCs into polymer matrixes by simple mixture often lead to the aggregation of NCs, resulting in the phase separation and the diminishing or quenching of the embedded NC luminescence [24]. To improve the compatibility between NCs and polymer matrices, the introduction of covalent bonds between the NCs surface and the polymer could be one of the most efficient methods, and presented as follows are two representative approaches: covalent attachment of presynthesized end-functionalized polymers to a reactive surface ("grafting to") [25], and in situ monomer polymerization with monomer growth of polymer chains from immobilized initiators ("grafting from") [26].

Catalytic chain transfer polymerization (CCTP) process is a well-proved powerful route to a relative low-molecular

weight polymer chain with a terminal double bond via free radical polymerization [27–30]. This process involves small amounts of the catalytic chain transfer agent, certain low-spin Co(II) complex in most cases, to catalyze the chain transfer to monomer reaction under oxygen-free condition. It is believed currently that the polymeric chains are initiated by a hydrogen atom, terminated by a vinyl end group, and suitable for further reaction via free radical polymerization. Despite their rare application in NC-polymer hybrid system before, the oligomers with anchors prepared by CCTP process would play good stabilizers. These vinyl end functionalized polymer ligands grafted on the surface of NCs could be further cross-linked to seal each NC in the closing network, therein obtaining well-stabilized NC-polymer hybrids. Recently, we reported the first example of NC-polymer hybrids with enhanced luminescence via CCTP process [31]. In an effort to extend this interesting field, we employed the CCTP process to synthesize a series of covalently linked CdS-polymer hybrid nanocomposites by in situ polymerization (i.e. "grafting from") or by "grafting to" approach and intramolecular cross-linking reaction. Describe herein are the preparation, characterization, and optical properties of CdS-polymer hybrid nanocomposites via CCTP, as well as the mechanism and kinetic investigation of the catalytic chain transfer reaction in the situ polymerization process.

Experimental section

Materials All manipulations were carried out under an atmosphere of purified nitrogen using standard Schlenk techniques. All reagents were of analytical grade and commercially available. Methyl methacrylate (MMA) was neutralized by 10 wt.% NaOH solution and then distilled under reduced vacuum to remove inhibitor. 2,2-azobis isobutyronitrile (AIBN) was recrystallized from ethanol twice and used as initiator. The cobalt catalyst bis(aqua)bis ((difluoroboryl)-dimethylglyoximato)cobalt(II) (CoBF) was prepared as described by Bakac and Espenson [32], and further confirmed by elemental analysis (Anal. Calcd. for $C_8H_{12}N_4O_4B_2F_4Co{\cdot}2H_2O$ (%): C, 22.84; N, 13.32; H, 3.83. Found: C, 22.86; N, 13.40; H, 3.89.). The monomer MMA and toluene for catalytic chain transfer polymerization were purged with high purity N_2 (BOC Gas) for at least 2 h prior to use. Other chemicals were used as purchased.

Synthesis of hydroxyl-coated CdS nanocrystals Hydroxyl-coated CdS nanocrystals were prepared according to the modified literature method [33]. A solution of $CdCl_2{\cdot}2.5H_2O$ (1.142 g, 5 mmol) in 3 mL of deionized water was mixed with a solution of 2-mercaptoethanol (ME; 0.781 g, 10 mmol) in 30 g of dimethylformamide (DMF). The mixture was vigorously stirred for 10 min. Three milliliters aqueous solution of $Na_2S{\cdot}9H_2O$ (0.721 g, 3 mmol) was then added dropwise slowly with continuous stirring. This treatment immediately led to a yellow and cloudy solution, which was stirred vigorously at room temperature for additional 4 h and subsequently formed a transparent yellow solution. The resulting solution was dehydrated by distillation under high vacuum, along with the addition of fresh DMF to keep the concentration of the solution. This stage was repeated twice. During the process of dehydration, the insoluble NaCl was precipitated and then removed by centrifugation. Transparent hydroxyl-coated CdS NCs suspension was finally obtained.

Surface modification of CdS nanocrystals with MPS To the hydroxyl-coated CdS NCs suspension obtained from the above step in DMF was added dropwise the stoichiometric methacryloxypropyltrimethoxysilane (MPS) (CdS NCs: MPS=4:3 wt/wt). The mixture was heated at ca. 110°C for 12 h under an atmosphere of N_2 with vigorous stirring and then cooled to room temperature. MPS-tethered CdS (CdS-MPS) NCs were precipitated by addition of toluene and acetone, separated, and then dried overnight under vacuum at room temperature.

Synthesis of CdS-PMMA hybrids in toluene via CCTP process The catalyst solution was prepared by dissolving 3 mg of CoBF into 25 g of the MMA monomer. CdS-MPS NCs powder (0.6 g) was dispersed in 60 mL of toluene solution containing AIBN (0.15 g) under N_2 atmosphere with continuous stirring. After evacuating and purging with high purity nitrogen six times, the solution was heated to 60°C, at which 28.2 g of deoxygenated MMA solution (30 mL) containing the desired amount of the catalyst solution (0, 0.3, 0.6, 1.2, and 2.4 g, respectively) was added dropwise. After stirring for 0.5 h, the mixture was cooled in an ice-water bath. Finally, CdS-polymethylmethacrylate (PMMA) hybrids were precipitated by addition of methanol, separated by centrifugation, and then dried under vacuum at room temperature. The clear solution obtained from centrifuging process was dried under vacuum at room temperature to afford the residue for the gel permeation chromatography (GPC) and nuclear magnetic resonance spectra (NMR) analysis.

Synthesis of CdS-PMMA hybrids in DMF via CCTP process The desired amount of CdS-MPS NCs powder (0.15 and 0.0 g, respectively) was dispersed in 60 mL of deoxygenated DMF via ultrasonic method, followed by the addition of the mixture AIBN (0.150 g) and the deoxygenated MMA solution (28.2 g, 30 mL) containing 1.2 g of the catalyst solution (prepared ditto). The reaction was carried out as described above and terminated by injecting methanol (10 mL).

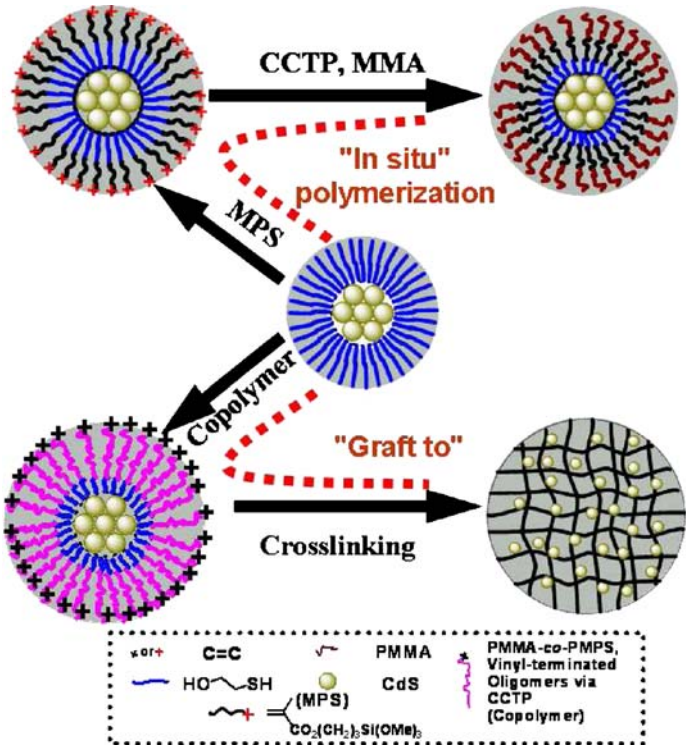

Scheme 1 Illustration of the routes for self-assembly of CdS-polymer hybrid nanocomposites

Synthesis of CdS-PMPS-*co*-PMMA hybrids and NCs network

Synthesis of PMPS-co-PMMA copolymer via CCTP process AIBN (0.150 g), MMA (30 mL), CoBF (0.30 mg), and MPS (3.498 g) were mixed in 60 mL of toluene. After evacuating and purging with high purity nitrogen six times, the mixture was heated at 70°C for 2 h under N_2 atmosphere with continuous stirring and then cooled immediately in an ice-water bath. The poly(methacryloxypropyltrimethoxysilane) (PMPS)-*co*-PMMA copolymer was precipitated by hexane, separated by centrifugation, and then dried under vacuum.

Synthesis of CdS-PMPS-co-PMMA hybrids and NCs network DMF solution containing hydroxyl-coated CdS NCs (1 wt.%), 2.25 g, was added dropwise to a solution of PMPS-*co*-PMMA (0.30 g) macromonomer in 37.45 g of DMF with continuous stirring. The mixture was stirred for 2 h at room temperature to afford CdS-PMPS-*co*-PMMA hybrids. Then a solution of AIBN in DMF was added dropwise to a proper amount of as-prepared CdS-PMPS-*co*-PMMA hybrids suspension with vigorous stirring under nitrogen atmosphere at 80°C for 4 h (AIBN, 0.25 wt.% of polymer ligands). CdS-PMPS-*co*-PMMA NCs network was prepared using intramolecular cross-linking reaction between the polymer ligands via free radical polymerization.

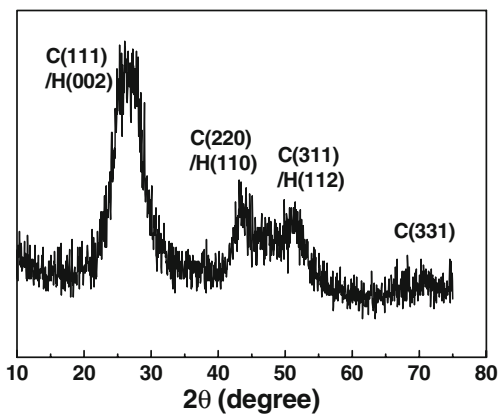

Fig. 1 XRD patterns of hydroxyl-coated CdS NCs

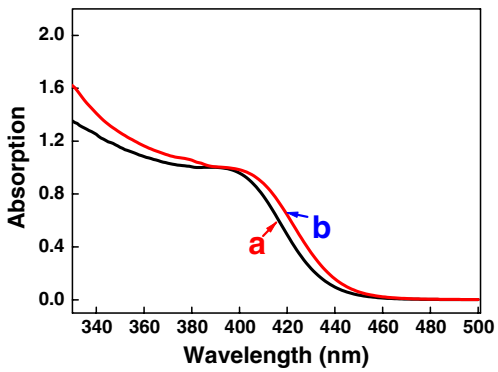

Fig. 2 UV-vis absorption spectra of (*a*) hydroxyl-coated CdS NCs (ME/Cd^{2+}/S^{2-}=2:1:0.6 mol/mol, H_2O/DMF=1:5 wt/wt) and (*b*) CdS-MPS NCs (CdS NCs/MPS=4:3 wt/wt)

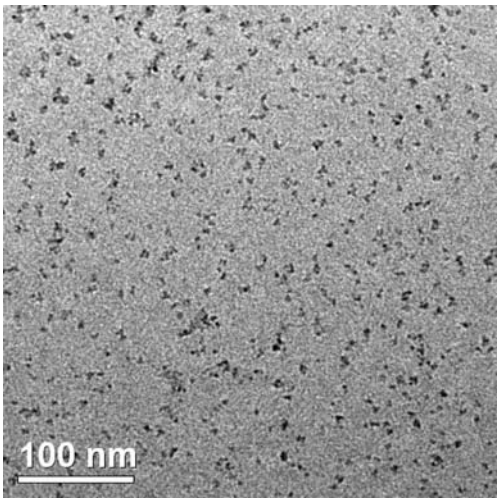

Fig. 3 TEM images of hydroxyl-coated CdS NCs dispersed in DMF (ME/Cd^{2+}/S^{2-}=2:1:0.6 mol/mol, H_2O/DMF=1:5 wt/wt, and reaction time=4 h)

Characterization Ultraviolet-visible (UV-vis) absorption spectra were recorded on a Perkin-Elmer Lambda 900 UV-vis spectrometer in the 300–500 nm region in DMF solution. Transmission electron microscope (TEM) images were collected by using a JEOL JEM-2100 electron microscope. Samples were dispersed in DMF and a drop of the solution was placed on a copper grid that was left to dry before transferring into the TEM sample chamber. The X-ray diffraction (XRD) patterns were conducted on Bruker-AXS D8 ADVANCE X-ray diffractometer with CuKα radiation (λ=0.1542 nm) at a scanning speed of 6°/min over 2θ range of 10–80°. Fourier transform infrared spectra (FT-IR) were recorded on a Nicolet 6700 FTIR spectrometer with KBr pellets in the 400–4,000 cm^{-1} region at a resolution of 4 cm^{-1} (32 scans). FT-Raman spectroscopy was performed on a NXR FT-Raman Module by sharing interferometer installed in the FT-IR bench. The Raman optics system is comprised of Nd:YVO_4 laser operating at 1,064 nm, sample holders, an InGaAs detector, and a CaF2 beam splitter. Spectra of fine powder samples pressed in a suitable sample holder were then collected with a laser power of 1.0 W, a mirror velocity of 0.3165 cm s^{-1}, and 128 scans at a resolution of 8 cm^{-1}. All the samples for the measurements of FT-IR and FT-Raman were required to wash and precipitate for several times for removal of all free PMMA polymers. The nuclear magnetic resonance spectra were measured on a Bruker AM 500 spectrometer in $CDCl_3$ solution. Photoluminescence (PL) spectra were obtained on a Varian Cary Eclipse spectrofluorometer with 340 nm laser beam as a light source. Molecular weight distributions were analyzed by gel permeation chromatography using a Waters 1515 isocratic pump, a Waters 717 plus autosampler, a column set consisting of three Waters Styragel® columns (7.8×300 mm) HR4, HR3, HR1, and a Waters 2414 differential refractive index detector. Tetrahydrofuran (TEDIA, HPLC grade) was used as eluent at 0.6 mL/min. Calibration of the GPC equipment was carried out with narrow polystyrene standards (Shodex® Standard, peak molecular weights rang 1,200–538,000).

Results and discussion

Synthesis and characterization In this paper, a series of CdS-polymer hybrid nanocomposites have been synthesized with the CCTP process. As shown in Scheme 1, hydroxyl-coated CdS nanocrystals with diameter of ca. 5 nm were firstly prepared with use of 2-mercaptoethanol (ME) as organic ligand. After surface treatment by methacryloxypropyltrimethoxysilane, CdS-PMMA hybrid nanocomposites were obtained via CCTP in situ (the upper section of Scheme 1). Moreover, PMPS-*co*-PMMA copolymer containing many anchors and a terminal double bond functional group was prepared by CCTP process. The incorporation of hydroxyl-coated CdS NCs into PMPS-*co*-PMMA matrices with covalent linkage afforded CdS-PMPS-*co*-PMMA hybrids, which were further intra-

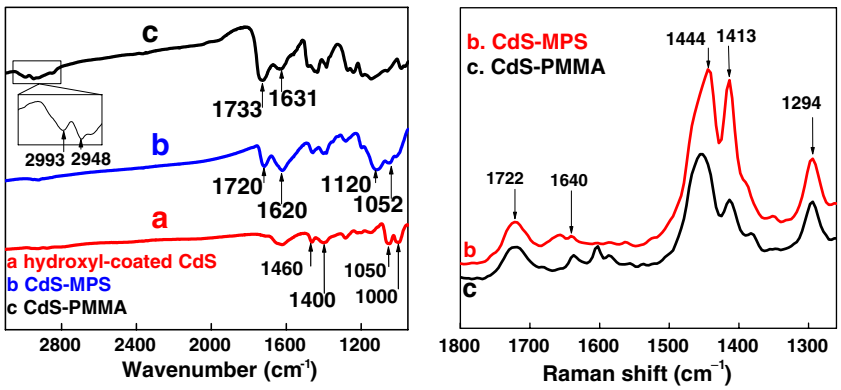

Fig. 4 FT-IR (*left*) and Raman (*right*) spectra of (*a*) hydroxyl-coated CdS NCs (ME/Cd^{2+}/S^{2-}=2:1:0.6 mol/mol, H_2O/DMF=1:5 wt/wt), (*b*) CdS-MPS NCs (CdS NCs/MPS=4:3 wt/wt) and (*c*) CdS-PMMA hybrids (CdS-MPS=0.60 g, AIBN=0.150 g, toluene=60 mL, MMA=30 mL, CoBF=0.24 mg). The *inset* shows the expanded IR spectra of 2,900–3,100 cm^{-1} region

Scheme 2 A probable mechanism for the in situ polymerization on the surface of modified CdS nanocrystals via CCTP

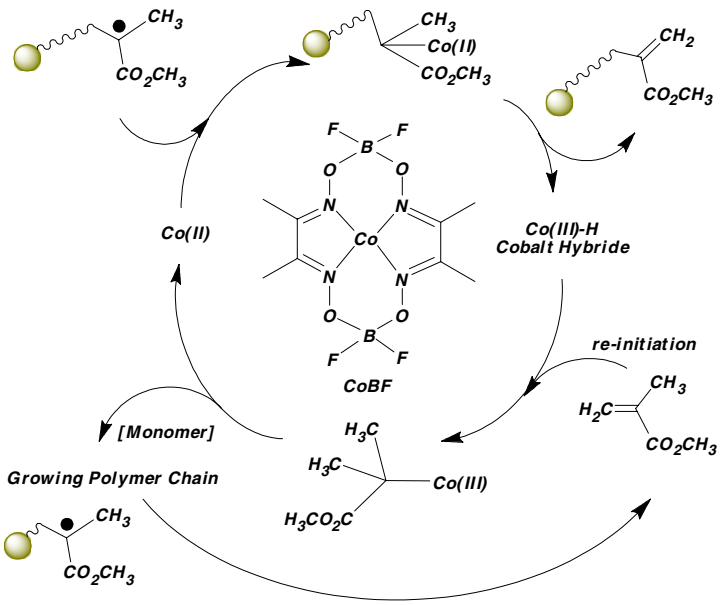

molecular cross-linked by free radical polymerization to form CdS NC-polymer network (the lower section of Scheme 1). The syntheses of NC-polymer hybrids were carried out in the presence of premade nanoparticles, providing full synthetic control over both the NCs and polymer matrices.

Hydroxyl-coated CdS NCs in DMF were prepared from $CdCl_2$ and Na_2S with the use of mercaptoethanol (ME) as capping ligand. The powder XRD of CdS NCs shown in Fig. 1 displays weak broad peaks, which is a typical characteristic of nanocrystals bearing small particle size [34–36]. The analysis of the XRD patterns reveals the coexistence of cubic and hexagonal phases in the CdS nanocrystal structure, which has also been discovered previously [35–37]. According to the Scherrer equation [35], the mean particle size is estimated from the XRD line width to be 5.7 nm, which is comparable to the data of 4.48 nm estimated from the UV-Vis absorption spectrum by Brus equation [38] (Fig. 2 (a)) and ca. 5 nm measured from transmission electron microscopy image (Fig. 3). The results indicate that as-prepared CdS NCs are well-dispersed in DMF solution and behave as quantum dots. In the FT-IR spectra (Fig. 4 (a)), the absorption bands at 1,050 cm^{-1} and 1,000 cm^{-1} (ν C–O) indicate hydroxyl groups are tethered on the surface of CdS NCs [39], while the absorption bands at 1,460 cm^{-1} is mainly due to the asymmetric bending vibrations of the methylene groups. Moreover, there is no characteristic absorption of the mercapto group, suggesting the free mercapto groups almost disappeared and the formation of robust bonding between Cd^{2+} and ME.

The condensation reaction of hydroxyl-coated CdS NCs with MPS yielded MPS-tethered CdS (CdS-MPS) NCs.

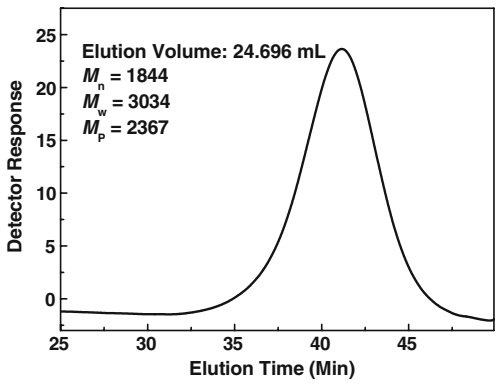

Fig. 5 Gel permeation chromatogram of PMPS-*co*-PMMA copolymer prepared with CoBF at 70 °C([MPS]/[MMA] = 1 : 20, [CoBF]/.([MMA] + [MPS]) = 2.73×10^{-6})

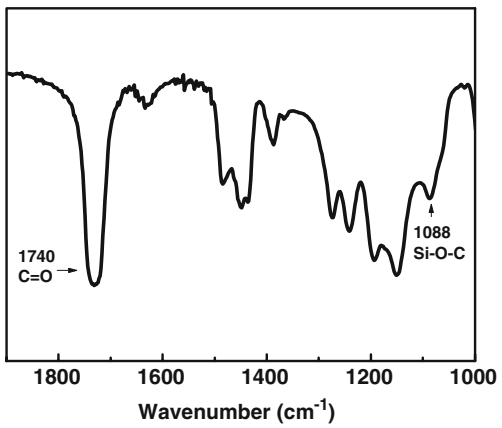

Fig. 6 FT-IR spectrum of PMPS-*co*-PMMA copolymer, [MPS]/[MMA] = 1 : 20, [CoBF]/([MMA] + [MPS]) = 2.73×10^{-6}

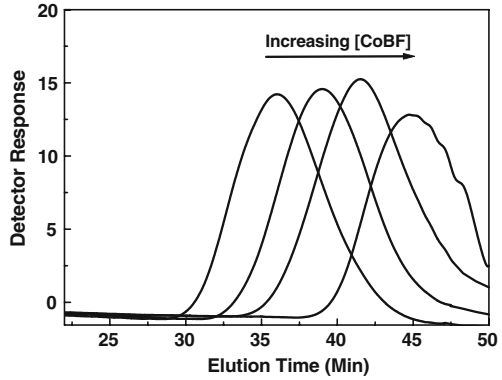

Fig. 7 Gel permeation chromatograms of PMMA prepared with the ratios of [CoBF]/[M] varying from 2.43×10^{-6} to 0

The insignificant shift of the absorption peak observed for CdS-MPS NCs in comparison with that of hydroxyl-coated CdS NCs suggests negligible change in the particle size of CdS NCs and it is still kept about 5 nm for CdS-MPS NCs (Fig. 2 (b)). Dangling double bonds on the surface of modified CdS nanocrystals allows of further covalent graft into PMMA matrix in situ and then CdS-PMMA hybrids were obtained based on CCTP process.

According to the well-established mechanism for catalytic chain transfer polymerization [30], we tried to investigate the in situ polymerization on the surface of modified CdS NCs via CCTP process, and a probable process for this system is presented in Scheme 2. Dangling double bonds on the surface of CdS-MPS NCs allows the polymerization of MMA in situ, initiated with AIBN, to afford growing radical chains. The chains are terminated by the Co(II) complex CoBF, yielding the dead polymers with vinyl end group, i.e. CdS-PMMA hybrids, and Co(III)H intermediates. The Co(III)H complex subsequently reacts with a monomer, MMA, to give the original Co(II) complex and a monomeric free radical for another in situ polymerization.

The FT-IR spectra of both CdS-MPS NCs and CdS-PMMA hybrids are shown in the left of Fig. 4. For CdS-MPS NCs, the absorption peaks at 1,052 cm^{-1} (ν Si–O–C) [40], 1,120 cm^{-1} (ν C–O–C) and 1,720 cm^{-1} (ν C=O) confirm the reaction of hydroxyl-coated CdS and MPS, while the strong absorption at 1,620 cm^{-1} (ν C=C) is indicative of the presence of double bonds. The characteristic absorptions of ester methyl (2,993 and 2,948 cm^{-1}) and carbonyl stretching vibrations (1,733 cm^{-1}) observed for CdS-PMMA hybrids suggest the surface-grafted PMMA nanocrystals are obtained via CCTP process. Moreover, the ν(C=O) and asymmetric ν(C=C) stretching vibrations of CdS-PMMA nanocomposites slightly shift to higher wavenumber with respect to those of MPS-CdS nanocrystals. This result is good agreement with the reported literature [22], which further confirms the occurrence of the reaction of PMMA with unsaturated terminal double bond groups of CdS-MPS nanocrystals.

The Raman spectra have been performed to verify the existence of double bonds in the as-prepared samples (the right of Fig. 4). The CH_2 ($–CH_2–$) deformation and in-plane twist vibrations in both samples are observed at 1,444 and 1,294 cm^{-1}, and the C=O stretching vibration occurs at 1,722 cm^{-1}. The absorptions at 1,640 and 1,413 cm^{-1} can be assigned to the C=C stretching and CH_2 ($R_2C=CH_2$) scissoring deformation vibrations, respectively; the former is stronger and the latter is weaker for CdS-PMMA hybrids compared with that of CdS-MPS NCs, which can be attributed to the enhanced steric effect after the graft reaction of PMMA onto the CdS-MPS. ^{1}H-NMR analysis of CdS-PMMA nanocomposites shows the peaks at δ 6.138 and 5.600, further confirming the formation of PMMA with terminal vinyl end group [41].

We have also successfully prepared covalently linked CdS-polymer hybrid nanocomposites by using "grafting to" method. Firstly, PMPS-*co*-PMMA copolymer (M_n=1,844) was obtained by the copolymerization of MPS and MMA via CCTP (Fig. 5). The characteristic absorption peaks of Si–O–C (1,088 cm^{-1}) and carbonyl vibration (1,740 cm^{-1}) indicate the successful occurrence of copolymerization of MPS and MMA (Fig. 6). Subsequently, the incorporation of the PMPS-*co*-PMMA ligand with hydroxyl-coated CdS

Table 1 Summary of molecular weight parameters of PMMA obtained from different ratios of [CoBF]/[M]

([CoBF]/[M])/10^{-6}	$M_n/10^3$	$M_w/10^3$	PDI
2.43	0.90	1.29	1.43
1.21	1.58	2.58	1.63
0.607	2.87	4.72	1.64
0.304	5.75	10.08	1.75

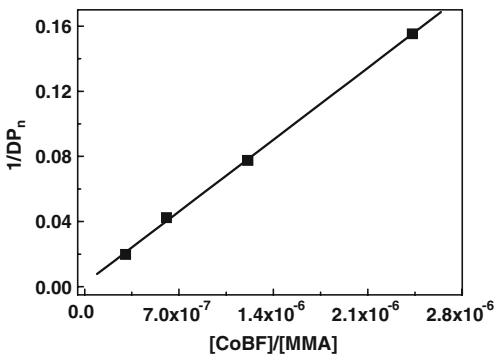

Fig. 8 Mayo plots of the polymerization of MMA with CoBF at 60°C based on $DP_n=M_w/(2m_0)$

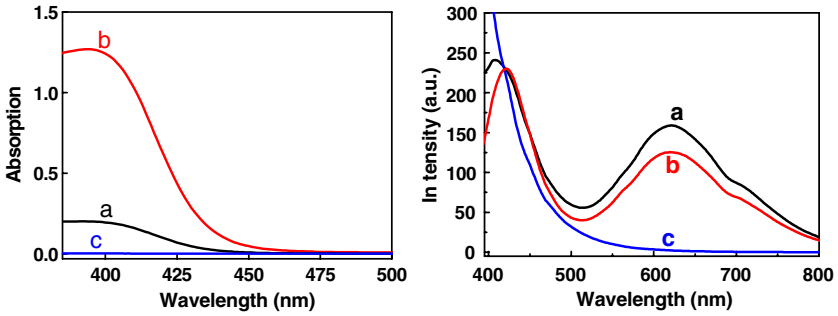

Fig. 9 The UV-vis absorption (*left*) and PL spectra (λ_{ex}= 340 nm; *right*) of (*a*) CdS-PMMA hybrids with the CdS-MPS/MMA ratio of 0.5 wt.%, (*b*) CdS-MPS NCs and (*c*) pure PMMA in DMF

NCs afforded CdS-PMPS-*co*-PMMA hybrids. The surface polymer ligands containing terminal double bonds were finally cross-linked to form CdS-PMPS-*co*-PMMA NCs network via free radical polymerization.

The kinetics of the catalytic chain transfer reaction in the situ polymerization process The resulting ungrafted PMMA in the situ polymerization process was used to determine the chain transfer constant of CoBF (C_s) of this free radical polymerization with Mayo equation (Eq. 1) [42, 43],

$$\frac{1}{DP_n} = \frac{1}{DP_{n,0}} + C_s \frac{[CoBF]}{[M]} \quad (1)$$

Where DP_n is the number average degree of polymerization and $DP_n = M_w/(2m_0)$ (M_w is the weight average molecular weight obtained from GPC and m_0 is the monomer mass), $DP_{n,0}$ is the average degree of polymerization in the absence of chain transfer agents, and [CoBF] and [*M*] are the concentration of catalyst and monomer respectively. A plot of DP_n^{-1}vs.[CoBF]/[*M*] should give a straight line with a slope equal to the chain transfer constant C_s. Five experiments were carried out with different ratios of [CoBF]/[*M*], in which [*M*] was kept constant and [CoBF] was varied. As shown in Fig. 7 and Table 1, the molecular weight distribution of PMMA shifts toward lower molecular weight with the increase in [CoBF], while all of the polymers show the similar polydispersity index (PDI≈1.6) which is consistent with that reported previously [44]. C_s was determined from the DP_n^{-1}vs.[CoBF]/[*M*] plot to be 6.30×10^4 (Fig. 8).

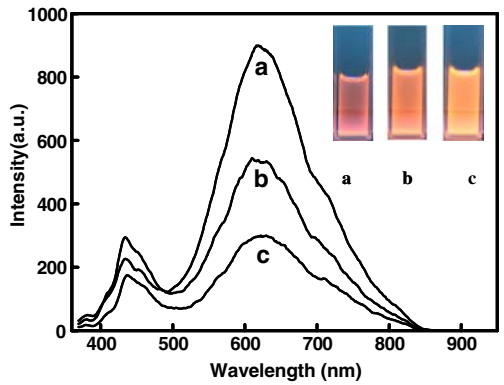

Fig. 10 The PL spectra excited at 340 nm of (*a*) CdS-PMPS-*co*-PMMA NCs network obtained from the intramolecular cross-linking reaction between CdS-PMPS-*co*-PMMA hybrids, (*b*) CdS-PMPS-*co*-PMMA hybrids and (*c*) hydroxyl-coated CdS NCs. The *inset* shows fluorescent photographs of the corresponding samples under 302 nm ultraviolet light

Optical properties of nanocrystal-polymer hybrids The UV-vis absorption and PL spectra of as-prepared CdS-PMMA hybrids recorded in DMF, along with those of CdS-MPS NCs and pure PMMA, are displayed in Fig. 9. There is no absorption peak for pure PMMA, while both CdS-MPS NCs and CdS-PMMA hybrids show an absorption peak at almost same position (at about 400 nm). These optical features indicate that surface capping essentially has no effect on the particle size of the inorganic nanocrystal cores, which is further corroborated by the insignificant shift of emission peaks observed for CdS-PMMA hybrids in comparison with that of CdS-MPS NCs. Therefore, the particle size of CdS NCs embedded in the PMAA matrix is still kept about 5 nm. As a typical semiconductor, CdS NCs display interesting optical properties. They exhibit characteristic emissions at 420 and 620 nm, which could be attributed to the recombination from the excitonic state in the particle interior and hole-electron recombination at surface traps, respectively [45, 46]. Moreover, an increase of PL intensity was observed after CdS NCs were embedded in the PMAA matrix, which can be ascribed to the local field enhancement effect [47]. These CdS nanocrystal cores were well-surrounded by dielectric polymer ligands which have much lower refractive indices than the inorganic semiconductors and hence bear a larger enhancement factor. Therefore, the boundary of different refractive indices between polymers and inorganic semiconductors resulted in the enhancement of PL.

CdS-PMPS-*co*-PMMA hybrids and NCs network exhibit characteristic emissions at about 450 and 620 nm (Fig. 10).

The PL intensity of the higher energy emission is much weaker than that of the lower energy emission, so the fluorescent color is dominated by the emission at 620 nm and it turned out to be orange under UV irradiation (the inset in Fig. 10). Perhaps most interestingly, the intramolecular cross-linking interaction between the polymer ligands on the surface of as-prepared nanocrystal can induce apparent fluorescence enhancement. As shown in Fig. 10, the PL intensity of CdS-PMPS-*co*-PMMA hybrids after cross-linking between all surface polymer ligands increases significantly with a near-twofold of increase of the relative intensity of the PL peak. We attribute this PL enhancement to a typical characteristic structure of these capping polymer ligands which contain terminal unsaturated double bonds. The local field enhancement effect should be one of the causes for the PL enhancement. In addition, the intramolecular cross-linking of the polymer ligands on the surface of each nanocrystal via multivalent interaction can seal each CdS NC in the ring-closing loops. The immobilization of the particles would lower diffusion quenching and thus intensify the PL. The cross-linking further enhances the relative cumulation density of CdS NCs compared with the control samples without cross-linking interaction. Since the amounts of photocurrents are controlled by the density of CdS particles [48], this enhancement of the density of CdS NCs by aid of cross-linking between them should also result the corresponding PL brightening.

Conclusions

This work demonstrates two new facile strategies to synthesize transparent CdS-polymer hybrid nanocomposites via catalytic chain transfer polymerization process. The covalent attachment of versatile polymer ligands on the surface of the NCs can efficiently seal each NC cluster in the polymer matrices. Moreover, NC-polymer network could be further formed by chemical cross-linking interaction between terminal double bonds of the low-molecular weight polymer ligands on the surface of NCs. The results show that surface capping has no essential effect on the particle size of the inorganic NC cores but leads to the luminescent enhancement. These available strategies can be applied widely to the fabrication of various NC-polymer nanocomposites containing such as CdS, ZnS, or core/shell nanoparticles. Hence, systemic research on synthesis of high-quality fluorescent NC-polymer hybrid nanocomposites via CCTP technique will continue.

Acknowledgments This work was supported by Natural Science Foundations (NSFs) of China (Grant No. 20576053, 20606016), NSF (NASA) of China (Grant No. 10676013), "863" Important National Science & Technology Specific Project (Grant No. 2007AA06A402), and the NSF of the Jiangsu Higher Education Institutions of China (Grant No. 07KJA53009).

References

1. Brus LE (1984) J Chem Phys 80:4403
2. Alivisatos AP (1996) Science 271:933
3. Tang ZY, Kotov NA, Giersig M (2002) Science 297:237
4. Peng XG, Thessing J (2005) Struc Bond 118:79
5. Coe S, Woo WK, Bawendi M, Bulovic V (2002) Nature 420:800
6. Tesster N, Medvedev V, Kazes M, Kan S, Banin U (2002) Science 295:1506
7. Mamedov AA, Belov A, Giersig M, Mamedova NN, Kotov NA (2001) J Am Chem Soc 123:7738
8. Huynh WU, Dittmer JJ, Alivisatos AP (2002) Science 295:2425
9. Wang L, Liu YS, Jiang X, Qin DH, Cao Y (2007) J Phys Chem C 111:9538
10. Huang MH, Mao S, Feick H, Yan HQ, Wu YY, Kind H, Weber E, Russo R, Yang PD (2001) Science 292:1897
11. Bruchez MJ, Moronne M, Gin P, Weiss S, Alivisatos AP (1998) Science 281:2013
12. Fernandez-Arguelles MT, Yakovlev A, Sperling RA, Luccardini C, Gaillard S, Sanz Medel A, Mallet JM, Brochon JC, Feltz A, Oheim M, Parak WJ (2007) Nano Lett 7:2613
13. Wang LY, Li P, Zhuang J, Bai F, Feng J, Yan XY, Li YD (2008) Angew Chem Int Ed 47:1054
14. Wang CW, Moffitt MG (2004) Langmuir 20:11784
15. Zhang H, Wang CL, Li MJ, Zhang JH, Lu G, Yang B (2005) Adv Mater 17:853
16. Sanchez-Gaytan BL, Cui W, Kim Y, Mendez-Polanco MA, Duncan TV, Fryd M, Wayland BB, Park SJ (2007) Angew Chem Int Ed 46:9235
17. Stavrinadis A, Beal R, Smith JM, Assender HE, Watt AAR (2008) Adv Mater 20:3105
18. Smith AM, Nie S (2008) J Am Chem Soc 130:11278
19. Chen Y, Thakar R, Snee PT (2008) J Am Chem Soc 130:3744
20. Bhaviripudi S, Qi J, Hu EL, Belcher AM (2007) Nano Lett 7:3512
21. Chen S, Zhu J, Shen YF, Hu CH, Chen L (2007) Langmuir 23:850
22. Chen L, Zhu J, Li Q, Chen S, Wang YR (2007) Eur Polym J 43:4593
23. Hwang SH, Moorefield CN, Wang P, Jeong KU, Cheng SZD, Kotta KK, Newkome GR (2006) J Am Chem Soc 128:7505
24. Cao XD, Li CM, Bao HF, Bao QL, Dong H (2007) Chem Mater 19:3773
25. von Werne T, Patten TE (2001) J Am Chem Soc 123:7497
26. Spange S (2000) Prog Polym Sci 25:781
27. Heuts JPA, Kukulj D, Forster DJ, Davis TP (1998) Macromolecules 31:2894
28. Heuts JPA, Forster DJ, Davis TP (1999) Macromol Rapid Commun 20:299
29. Heuts JPA, Forster DJ, Davis TP (1999) Macromolecules 32:3907
30. Gridnev AA, Ittel SD (2001) Chem Rev 101:3611
31. Yang SY, Li Q, Chen L, Chen S (2008) J Mater Chem 18:5599
32. Bakac A, Espenson JH (1984) J Am Chem Soc 106:5197
33. Nosaka Y, Yamaguchi K, Miyama H, Hayashi H (1988) Chem Lett 17:605
34. Zhang H, Zhou Z, Yang B, Gao MY (2003) J Phys Chem B 107:8
35. Ghosh S, Mukherjee A, Kim H, Lee C (2003) Mater Chem Phys 78:726
36. Chen M, Pan LJ, Huang ZQ, Cao JM, Zheng YD, Zhang HQ (2007) Mater Chem Phys 101:317

37. Wang SH, Yang SH, Yang CL, Li ZQ, Wang JN, Ge WK (2000) J Phys Chem B 104:11853
38. Brus L (1986) J Phys Chem 90:2555
39. Lue CL, Cui ZC, Li Z, Yang B, Shen JC (2003) J Mater Chem 13:526
40. Jing SY, Lee HJ, Choi CK (2002) J Korean Phys Soc 41:769
41. Haddleton DM, Depaquis E, Kelly EJ, Kukulj D, Morsley SR, Bon SAF, Eason MD, Steward AG (2001) Polym Chem 39:2378
42. Mayo FR (1943) J Am Chem Soc 65:2324
43. Roberts GE, Davis TP, Heuts JPA, Russell GT (2002) Polym Chem 40:782
44. Suddaby KG, Maloney DR, Haddleton DM (1997) Macromolecules 30:702
45. Chestnoy N, Harris TD, Hull R, Brus LE (1986) J Phys Chem 90:3393
46. Noglik H, Pietro WJ (1994) Chem Mater 6:1593
47. Wang Y, Herron N (1991) J Phys Chem 95:525
48. Torimoto T, Tsumura N, Miyake M, Nishizawa M, Sakata T, Mori H, Yoneyama H (1999) Langmuir 15:1853